

DR. TAIHAO QUAN (Orcid ID : 0000-0002-0954-5109)

Article type : Original Article

**Actin cytoskeleton assembly regulates collagen production via TGF- $\beta$  type II receptor in human skin fibroblasts**

Zhaoping Qin, Gary J. Fisher, John J. Voorhees, Taihao Quan\*

Department of Dermatology, University of Michigan Medical School, Ann Arbor, Michigan, USA

\*To whom correspondence should be addressed:

Department of Dermatology

University of Michigan Medical School

1301 E. Catherine, Medical Science I, Room 6447

Ann Arbor, Michigan 48109-5609

Telephone: (734) 615-2403

Facsimile: (734) 647-0076

e-mail: [thquan@umich.edu](mailto:thquan@umich.edu)

**Running Title:** Cytoskeleton disassembly impairs TGF- $\beta$  signaling

This is the author manuscript accepted for publication and has undergone full peer review but has not been through the copyediting, typesetting, pagination and proofreading process, which may lead to differences between this version and the [Version of Record](#). Please cite this article as [doi: 10.1111/jcmm.13685](https://doi.org/10.1111/jcmm.13685)

This article is protected by copyright. All rights reserved

**Abbreviations:** T $\beta$ RII, TGF- $\beta$  type II receptor; CCN2, connective tissue growth factor; ECM, extracellular matrix; Lat-A, latrunculin-A; microRNA 21, miR-21

## **Abstract**

The dermal compartment of skin is primarily composed of collagen rich extracellular matrix (ECM), which is produced by dermal fibroblasts. In Young skin, fibroblasts attach to the ECM through integrins. During aging, fragmentation of the dermal ECM limits fibroblast attachment. This reduced attachment is associated with decreased collagen production, a major cause of skin thinning and fragility, in the elderly. Fibroblast attachment promotes assembly of the cellular actin cytoskeleton, which generates mechanical forces needed for structural support. The mechanism(s) linking reduced assembly of the actin cytoskeleton to decreased collagen production remains unclear. Here we report that disassembly of the actin cytoskeleton results in impairment of TGF- $\beta$  pathway, which controls collagen production, in dermal fibroblasts. Cytoskeleton disassembly rapidly down-regulates TGF- $\beta$  type II receptor (T $\beta$ RII) levels. This down-regulation leads to reduced activation of downstream effectors Smad2/Smad3 and CCN2, resulting in decreased collagen production. These responses are fully reversible; restoration of actin cytoskeleton assembly up-regulates T $\beta$ RII, Smad2/Smad3, CCN2, and collagen expression. Finally, actin cytoskeleton-dependent reduction of T $\beta$ RII is mediated by induction of microRNA-21, a potent inhibitor of T $\beta$ RII protein expression. Our findings reveal a novel mechanism that links actin cytoskeleton assembly and collagen expression in dermal fibroblasts. This mechanism likely contributes to loss of T $\beta$ RII and collagen production, which are observed in aged human skin.

**Key words:** Cytoskeleton, Collagen, TGF- $\beta$  signaling, Skin aging, Extracellular matrix

## **Introduction**

Loss of tissue mass and accumulation of tissue damage are common features of aging of many vital tissues [1,2]. In human skin, these age-associated features are readily observable as thinning and fragility. The dermal extracellular matrix (ECM), which is composed primarily of type I collagen fibrils, provides the majority of skin mass, and is responsible for structural/mechanical support [3]. Increased fragmentation and reduced production of type I collagen fibrils are prominent features of the skin dermis in aged individuals [4-9]. Age-

associated alterations of collagen fibrils also create a tissue microenvironment that compromises skin health by impairing vasculature function [2,10,11], delaying wound healing [12-14], and promoting skin cancer [15,16].

In skin, fibroblasts are primarily responsible for synthesis of the dermal ECM. In young healthy skin, dermal fibroblasts attach to intact, dense collagen fibrils, through integrin collagen receptors. This attachment promotes assembly of the cellular actin cytoskeleton, which generates mechanical forces that give rise to fibroblast morphology [6,17-20]. During aging, collagen fibrils become fragmented, less dense, and disorganized [17]. Fragmentation destroys attachment sites, thereby diminishing the assembly of the actin cytoskeleton within fibroblasts.

Assembly of the actin cytoskeleton, following integrin-dependent attachment of fibroblasts to the dermal ECM, is a highly complex process involving the coordinated assembly of a large number of cytoskeletal proteins. Central to this process is the dynamic, reversible polymerization of actin monomers to form microfilaments that provide critical intracellular mechanical support [28-30].

Production of ECM proteins by dermal fibroblasts is primarily regulated by the TGF- $\beta$  pathway. The actions of TGF- $\beta$  are mediated by a cell surface receptor complex, composed of type I and type II TGF- $\beta$  receptors, and downstream effector Smad proteins (Smad2, 3 and 4), which are transcription factors. Smad proteins regulate many genes that encode for components of the ECM, including collagens, laminins, fibronectin, and proteoglycans [5,9,31]. In aged human skin, several components of the TGF- $\beta$  pathway are reduced [9,32]. Impairment of the TGF- $\beta$  pathway like accounts, at least in part, for diminished ECM production that is observed in aged skin

In this study, we used latrunculin A (Lat-A), a potent inhibitor of actin [33,34], to investigate mechanisms that link assembly of actin microfilaments to production of type I collagen, in human skin fibroblasts. We find that interference with actin polymerization impairs the TGF- $\beta$  signaling pathway through specific down-regulation of TGF- $\beta$  type II receptor (T $\beta$ RII). This down-regulation is mediated, in part, by increased microRNA 21 (miR-21), which directly targets T $\beta$ RII synthesis. These data provide novel insights into mechanisms by which disassembly of the actin cytoskeleton may deleteriously alter fibroblast function leading to age-associated skin atrophy.

## **Materials and methods**

### **Materials**

MEM  $\alpha$ , GlutaMAX™, Fetal Bovine Serum (FBS), 0.25% trypsin-EDTA solution and Penicillin-Streptomycin were purchased from GIBCO/Thermo Fisher (Wayne, MI, USA). Collagen I (rat tail) was obtained from BD Biosciences (Palo Alto, CA, USA). TGF- $\beta$ 1 was obtained from R&D Systems (Minneapolis, MN, USA). Latrunculin A was obtained from Enzo Life Sciences (Farmingdale, NY, USA). T $\beta$ RII siRNA (AACGGTGCAGTCAAGTTTCCA) and miR-21 mimic (TAGCTTATCAGA-CTGATGTTGA) were purchased from Qiagen (Chatsworth, CA, USA). miR-21 inhibitor (CAACATCAGTCTGATAAGCT) was purchased from EXIQON (Woburn, MA, USA). All other reagents were purchased from Sigma Chemical Company (St. Louis, MO, USA).

### **Cell culture**

Primary adult human dermal fibroblasts were prepared from full-thickness punch biopsies (4 mm) obtained from sun-protected buttock skin of healthy adult human volunteers (mean age 35 $\pm$ 5 years). Dermal fibroblasts were isolated from skin biopsies by digestion with bacterial collagenase (Worthington Biochemical Corporation, Lakewood, NJ, USA). Early passage (less than 9 passages) dermal fibroblasts were cultured in MEM  $\alpha$ , GlutaMAX™ with 10% Fetal Bovine Serum (FBS) at incubator with 37°C, 5% CO<sub>2</sub>. Three-dimensional (3D) collagen gels were made following a previous publication with minor modification [17]. Briefly, neutralized rat tail type-I collagen was mixed in cocktail (DMEM, NaHCO<sub>3</sub> [44 mM], L-glutamine [4 mM], Folic Acid [9 mM], and neutralized with 1N NaOH to pH 7.2). Fibroblasts (0.5x10<sup>6</sup>) were suspended in 2 ml collagen and medium cocktail solution then plated in 35 mm bacterial culture dishes. After collagen polymerization, collagen gels were incubated with 2 ml media (DMEM, 10% FBS) at 37°C, 5% CO<sub>2</sub>. For latrunculin-A (Lat-A) experiment, cells were treated with Lat-A (30 nM) for 24 hours.

### **RNA isolation and quantitative real-time RT-PCR**

Total RNA was extracted using Trizol reagent (Invitrogen). cDNA was prepared by reverse transcription of total RNA(100ng) using a Taqman Reverse Transcription Reagents (Applied Biosystems, Foster City, CA, USA). Real-time PCR was performed on a 7300 Real-Time PCR System (Applied Biosystems) using SYBR Green PCR Master Mix (Applied Biosystems). Type I procollagen, CCN2, and T $\beta$ RII primers were purchased from Applied Biosystems. Target gene mRNA expression levels were normalized to the house keeping gene 36B4 for quantification.

miR-21 levels were determined by real-time PCR using TaqMan® MicroRNA Assays Kit (Life Technology, NY, USA) following the manufacturer's instructions.

### **Western analysis**

Western blots were performed as described previously [35]. Briefly, whole cell proteins were prepared by using whole cell lysis buffer followed by centrifugation. Equal amount of proteins (50µg/lane) were analyzed for each sample by resolving on 10% SDS-PAGE. The SDS gels were transferred to PVDF membrane; the membranes were blocked with 5% milk-TBST for one hour at room temperature, followed by incubation with primary antibodies for one hour at room temperature. Primary antibodies: type I collagen (Southern Biotech, Birmingham, AL, USA), CCN2 (SC-14939, L20, Santa Cruz Biotechnology, Santa Cruz, CA, USA), TβRI (SC-398, V-22, Santa Cruz Biotechnology), TβRII (SC-400, L-21, Santa Cruz Biotechnology), and total and phospho-Smad3 (Cell Signaling Technology, Danvers, MA, USA). The membranes were washed with TBST then incubated with corresponding secondary antibodies for one hour at room temperature. Followed by three times TBST washing, the blots were incubated in ECF (Vistra ECF Western Blotting System, Amersham Pharmacia Biotech, Piscataway, NJ, USA) following the manufacturer's instructions. The blots were scanned by STORM MolecularImager (Molecular Dynamics, Sunnyvale, CA, USA). The intensities of each band were quantified using ImageQuant (GE HealthCare, Piscataway, NJ) and normalized using β-actin as a marker for equal protein loading.

### **ProteinSimple capillary electrophoresis immunoassay**

In some experiments, protein levels were determined by ProteinSimple capillary electrophoresis immunoassay. ProteinSimple capillary electrophoresis immunoassay overcomes many of the technical drawbacks of Western analysis, while providing much greater sensitivity, in the low nanogram range. ProteinSimple capillary electrophoresis immunoassay was performed according to the ProteinSimple manufacture's user manual. In brief, whole cell extract samples (800 ng/lane) were mixed with kit provided master mix. The mixture was then heated at 95°C for 5 minutes. The samples including primary antibodies, blocking reagent, HRP-conjugated secondary antibodies, chemiluminescent substrate, and separation and stacking matrices were also dispensed to designated wells plate according to the ProteinSimple manufacture's user manual. The electrophoresis, blocking, washing, and immunodetection steps took place in the capillary system (ProteinSimple Wes, ProteinSimple, Santa Clare, CA, USA) and were fully

automated with instrument default settings. Corresponding protein bands from digital images were identified based on the molecular weight. The intensities of each protein was analyzed by quantification with Compass software (ProteinSimple) after normalization by and  $\beta$ -actin (loading control).

### **Transient transfection, immunostaining, and phalloidin staining**

Primary adult human dermal fibroblasts were transiently transfected with T $\beta$ RII expression vector [36] or siRNAs (T $\beta$ RII siRNA, miR-21 mimic, and inhibitor) by electroporation using human dermal fibroblasts nucleofector kit (Amaxa Biosystems, Gaithersburg, MD, USA). Immunocytochemistry was performed as described previously [9]. Briefly, cells were fixed in 4% PFA (paraformaldehyde) for two hours at room temperature, followed by incubation with 0.5% Nonidet P-40, blocking with 2% BSA (bovine serum albumin), washing with PBS five times/ the cells were then incubated with type I procollagen (Santa Cruz Biotechnology, Santa Cruz, CA, USA), CCN2 (SC-14939, L2, Santa Cruz Biotechnology), Phospho Smad3 (ab52903, abcam, Cambridge, MA, USA), T $\beta$ RII (SC-400, L-21, Lot #: A1516, Santa Cruz Biotechnology) primary antibodies for 1 hour at room temperature, followed by incubation with Super Sensitive MultiLink (BioGenex, Fremont CA, USA) for 10 minutes and streptavidin-conjugated AlexaFluor 594 or 488 (Invitrogen-Molecular Probes, San Diego, CA) for 10 minutes. Mounting medium with DAPI was added to stain cell nuclei. Corresponding IgG isotype (negative control) show no specific staining (data not shown). Phalloidin was used to stain cells morphology.

### **Statistical analysis**

Comparisons between samples were performed with the paired *t*-test (two groups) or the repeated measures of ANOVA (more than two groups). Multiple pair-wise comparisons among samples were made with the Tukey Studentized Range test. All *p* values are two-tailed, and considered significant when  $<0.05$ .

### **Results**

#### **Disassembly of actin cytoskeleton down-regulates TGF- $\beta$ type II receptor**

To explore the connection between the actin cytoskeleton and dermal fibroblast function, we disrupted the cytoskeleton with Lat-A, which sequesters monomeric actin thereby causing rapid depolymerization of actin microfilaments [37]. As expected, Lat-A caused marked loss of actin stress fibers (Figure 1a, left panel) and reduced the average surface area of fibroblasts approximately 70% (Figure 1a, right panel).

We previously reported that the TGF- $\beta$  pathway is regulated by cell size and mechanical force regulate in dermal fibroblasts [26]. When fibroblasts contract and generate less mechanical force, TGF- $\beta$  signaling is reduced [29]. Therefore, we investigated whether disassembly of the actin cytoskeleton, which reduces fibroblast size and mechanical force, alters gene expression of TGF- $\beta$  pathway components. Cytoskeletal disassembly did not alter levels of TGF- $\beta$  ligand TGF- $\beta$ 2, TGF- $\beta$  type I receptor (T $\beta$ RI), or downstream effector Smads, Smad2, Smad3, Smad4, or Smad7 (Figure 1b). In contrast, cytoskeletal disassembly increased gene expression of TGF- $\beta$  ligands TGF- $\beta$ 1 and TGF- $\beta$ 3, and reduced expression of TGF- $\beta$  type II receptor (T $\beta$ RII). This down regulation of T $\beta$ RII mRNA was accompanied by significant reduction of T $\beta$ RII protein (Figure 1c). T $\beta$ RII protein was significantly decreased by 78%.

### **Actin cytoskeleton disassembly down-regulates TGF- $\beta$ /Smad signaling and TGF- $\beta$ -regulated type I procollagen and CCN2 expression**

We next investigated the functional impact of actin cytoskeleton disassembly on TGF- $\beta$  signal transduction and target gene expression. Indeed, we found that TGF- $\beta$ -induced phosphorylation of the downstream effectors Smad2 and Smad3 was significantly inhibited by disassembly of the actin cytoskeleton (Figure 2a). Phosphorylation of Smad2/3 is necessary for TGF- $\beta$  regulation of target genes. For example, Smad3 activation is necessary for TGF- $\beta$  induction of two genes that are critical for ECM function, type I procollagen and CCN2 (connective tissue growth factor) [9]. Actin cytoskeleton disassembly significantly reduced expression of both target genes. TGF- $\beta$  induction of type I procollagen mRNA (Figure 2b) and protein (Figure 2c) was reduced 58% and 76%, respectively. TGF- $\beta$  induction of CCN2 mRNA (Figure 2d) and protein (Figure 2e) was reduced 72% and 80%, respectively.

Dermal fibroblasts reside within a three-dimensional (3D) collagen fibril-rich ECM microenvironment in human skin. Accordingly, we investigated the impact of actin cytoskeleton disassembly on type I procollagen and CCN2 expression in fibroblasts cultured within 3D collagen lattices. In 3D collagen cultures, consistent with monolayer culture (Figure 1a), depolymerization of the actin cytoskeleton resulted in decreased fibroblast surface area (Figure 2f, right panel), and reduced expression of type I procollagen and CCN2 mRNA (Figure 2g) and protein (Figure 2h).

### **Actin cytoskeleton assembly stimulates TGF- $\beta$ signaling and type I procollagen expression.**

Inhibition of actin microfibril formation by Lat-A has been shown to be rapidly reversible [38,39]. This reversibility provides a unique opportunity to control cytoskeletal assembly and determine its role in fibroblast functions. Therefore, we next assessed the impact of actin cytoskeleton assembly on TGF- $\beta$  signaling and gene regulation. For these studies, fibroblasts were first treated with Lat-A or vehicle for 24 hours, and then Lat-A-containing media were replaced with normal media. Within 24 hours after removal of Lat-A, distinct actin microfibrils were observed (Figure 3a). Importantly, T $\beta$ RII protein levels were also restored to pre-Lat-A treatment levels (Figure 3b). This restoration of T $\beta$ RII was associated with enhanced signal transduction, as demonstrated by increased TGF- $\beta$ -induced Smad2/Smad3 phosphorylation (Figure 3c). In addition, consistent with up-regulation of TGF- $\beta$  signaling, TGF- $\beta$  induction of both type I procollagen and CCN2 protein levels was significantly elevated (Figure 3d)

### **T $\beta$ RII downregulation mediates impaired TGF- $\beta$ signaling and type I procollagen production by actin cytoskeleton disassembly**

The above data indicate that the TGF- $\beta$  pathway is regulated by the state of actin cytoskeleton assembly and suggest that T $\beta$ RII is a critical mediator of this regulation. To investigate this possibility, we determined the impact of loss or gain of T $\beta$ RII. We confirmed that T $\beta$ RII siRNA efficiently reduced the expression of T $\beta$ RII and TGF- $\beta$ 1 induced Smad3 phosphorylation (Figure 4a). As expected, removal of Lat-A restored TGF- $\beta$  signaling (Figure 4, fourth panel from the left). In contrast, siRNA-mediated knockdown of T $\beta$ RII blocked restoration of TGF- $\beta$  signaling following removal Lat-A (Figure 4b, last panel). We also found that prevention of T $\beta$ RII down-regulation, by transfection of T $\beta$ RII expression vector, blocked down regulation of type I procollagen (Figure 4b, upper row) and CCN2 (Figure 4c, lower row) protein expression, following Lat-A-mediated actin cytoskeleton disassembly. In contrast, expression of T $\beta$ RII did not prevent Lat-A-mediated actin cytoskeleton disassembly (Figure 4d). These data demonstrate that modulation of T $\beta$ RII expression in response to the state of actin cytoskeleton assembly plays a key role in regulation of TGF- $\beta$  signaling and production of type I collagen and CCN2.

### **Reduction of fibroblast size *per se* does not down-regulate TGF- $\beta$ signaling or T $\beta$ RII**

Integrins are cell surface receptors that bind to the ECM and link the ECM to the intracellular actin cytoskeleton. Integrins thereby play a critical role in normal cell attachment,



and spreading [40,41]. Disassembly of the actin cytoskeleton reduces cell spreading. We investigated whether reduced fibroblast spreading, under conditions of integrin-independent cell attachment, exerts similar effects on TGF- $\beta$  signaling as reduced cell spreading due to cytoskeleton disassembly by Lat-A treatment. For these studies, dermal fibroblasts were cultured on poly-L-lysine coated surfaces, which allow integrin-independent attachment and spreading [42]. Under these conditions, fibroblasts displayed limited spreading and reduced cell surface area (Supplemental Fig 1a left panel), compared to cultures on uncoated, standard tissue culture plates (Supplemental Figure 1b left panel). Interestingly, this reduced spreading did not alter TGF- $\beta$ -induced Smad3 phosphorylation (Supplemental Figures 1a and 1b) or T $\beta$ RII expression (Supplemental Figure 1c), compared to fully spread fibroblasts.

To further explore the relationship between reduced fibroblast spreading and TGF- $\beta$  signaling, we examined cells at early times after attachment to standard tissue culture plates, prior to full spreading. Although fibroblasts displayed limited spreading at 30 and 60 minutes after attachment, compared to 24 hours after attachment, TGF- $\beta$ -induced Smad3 phosphorylation was similar at all time points.

#### **Actin cytoskeleton disassembly induces miR-21, which reduces T $\beta$ RII expression**

Finally, we explored the potential mechanism by which actin cytoskeleton disassembly reduces T $\beta$ RII expression. Several recent reports indicate that T $\beta$ RII expression is largely regulated by microRNA-21 (miR-21) in both stromal (adipose tissue-derived mesenchymal stem cells) and epithelial cells (colon cancer cell lines, HCT-116 and HT-29) [43,44]. miR-21 regulates T $\beta$ RII expression through direct interaction with the 3' non-translated region in the T $\beta$ RII transcript. Interestingly, we observed that actin cytoskeleton disassembly leads to significant induction of miR-21 levels (Figure 5a). Furthermore, we found that miR-21 mimic significantly down-regulated T $\beta$ RII protein level, whereas miR-21 inhibitor significantly increased T $\beta$ RII protein level in human dermal fibroblasts (Figure 5b). Importantly, blocking miR-21 induction by miR-21 inhibitor prevented suppression of T $\beta$ RII by actin cytoskeleton disassembly (Figure 5c). We also confirmed that miR-21 mimic inhibited Smad3 phosphorylation (Fig 5d and 5e) and reduced the expression of T $\beta$ RII, and TGF- $\beta$  target genes, type I collagen and CCN2 (Fig 5f).

## Discussion

Fibroblasts in young skin attach to dense, intact collagen fibrils, which compose the bulk of skin dermal ECM connective tissue. This attachment promotes assembly of the actin cytoskeleton and generation of mechanical force. During aging, dermal collagen fibrils become fragmented and disorganized [17,18,20]. This degeneration of the dermal ECM impairs fibroblast attachment and consequent assembly of the intracellular actin cytoskeleton. Decline of collagen production by fibroblasts is a prominent feature of skin aging [5,6,9,45]. Emerging evidence indicates that cell-substrate attachment and assembly of the actin cytoskeleton, play critical roles in diverse cellular biological processes, such as proliferation, differentiation, signal transduction, and gene expression. [22,23]. Here we explored the impact of disassembly of the actin cytoskeleton on the regulation of collagen production by dermal fibroblasts. Our results indicate that disassembly of actin cytoskeleton leads to down-regulation of collagen production via impairment of TGF- $\beta$ /Smad signaling. These data suggest that reduced assembly of the actin cytoskeleton in aged skin, due to fragmentation of collagen fibrils in the dermal ECM, may contribute to age-related collagen loss, in human skin.

The TGF- $\beta$ /Smad signaling pathway is a major regulator of ECM production [9,31,46,47].

TGF- $\beta$  initiates its biological actions through interactions with the TGF- $\beta$  receptor complex [48]. TGF- $\beta$  binding to T $\beta$ RII is required to initiate the TGF- $\beta$  signaling pathway. Binding of TGF- $\beta$  to T $\beta$ RII triggers its association with T $\beta$ RI, which phosphorylates and activates downstream Smad effectors. We found that actin cytoskeleton disassembly down-regulated T $\beta$ RII, without affecting T $\beta$ RI expression. Three distinct isoforms of TGF- $\beta$  ( $\beta$ 1,  $\beta$ 2, and  $\beta$ 3) have been identified in mammalian cells [49]. Although they are structurally homologous, TGF- $\beta$ 1 and TGF- $\beta$ 3 bind to T $\beta$ RII with higher affinity than TGF- $\beta$ 2 in most cells [50,51]. Cytoskeleton disassembly modestly induced TGF- $\beta$ 1 and TGF- $\beta$ 3. This induction may reflect a compensatory response to down-regulation of T $\beta$ RII. In skin fibroblasts, reduction of T $\beta$ RII, without reduction of T $\beta$ RI, results in loss of cellular binding of TGF- $\beta$  and impairment of downstream Smad signaling [52]. Thus, cytoskeleton disassembly impairs the first step of TGF- $\beta$  signaling by substantially reducing T $\beta$ RII expression.

The actin cytoskeleton plays a critical role in the maintenance of the structural integrity of the cell and diverse dynamic cellular functions. As such, disassembly of actin filaments affects

many cellular processes. Our data identify T $\beta$ RII expression as the major mechanism by which actin cytoskeleton assembly regulates collagen production. Actin cytoskeleton assembly is known to regulate other pathways, including Hippo signaling [53] and MRT/SRF dependent gene expression [28].

Integrins function as primary cell surface receptors for attachment of cells to the ECM. As such, integrins serve as physical links between the ECM and the intracellular actin cytoskeleton. Together, the actin cytoskeleton and integrins generate mechanical force. We found that limited fibroblast spreading, due to either integrin-independent cell attachment, or at early times after integrin-mediated attachment, does not reduce T $\beta$ RII or impair TFG- $\beta$  signaling (Supplemental Figures 1 and 2). These data support the conclusion that actin cytoskeletal disassembly, rather than reduced fibroblast spreading *per se*, down-regulates T $\beta$ RII, leading to reduced collagen production.

Interestingly, miR-21, a potent inhibitor of T $\beta$ RII expression [43,44], is induced by actin cytoskeleton disassembly, and mediates T $\beta$ RII down-regulation. These data suggest that expression of miR-21 may be regulated, in part, by cellular mechanical sensing mechanisms. The transcription factor activator protein 1 (AP-1) has been reported to directly regulate expression of miR-21 through several response elements in the miR-21 promoter [54]. We have previously reported that reduced mechanical force elevates AP-1 activity in human dermal fibroblasts [17], suggesting that miR-21 elevation in response to actin cytoskeleton disassembly may result from activation of AP-1. Additionally, we reported that reduced mechanical force increases reactive oxygen species (ROS), which induce AP-1 [55], in human dermal fibroblasts [17,56]. Interestingly, elevated ROS specifically down-regulates T $\beta$ RII, without affecting T $\beta$ RI [36]. These data support the possibility that actin cytoskeleton disassembly may upregulate miR-21 through ROS-mediated AP-1 activation, leading to down-regulation of T $\beta$ RII. Obviously, additional studies are needed to address the detailed molecular mechanism(s) of actin cytoskeleton-specific down-regulation of T $\beta$ RII expression.

We and others have previously shown that many TGF- $\beta$ /Smad-regulated ECM proteins are down-regulated in aged human skin [9,45]. Importantly, we observed down-regulation T $\beta$ RII in naturally aged [32], photoaged [32], and acute ultraviolet-irradiated human skin *in vivo* [52], with no change of T $\beta$ RI expression. These data indicate that T $\beta$ RII and T $\beta$ RI are differentially

regulated and that T $\beta$ RII specific down-regulation may play a key role in impaired TGF- $\beta$ /Smad signaling and reduced ECM synthesis that are observed in aged human skin.

Recently, we reported that enhancing mechanical support within the dermis by direct injection of dermal filler (cross-linked hyaluronic acid) into aged human skin *in vivo* increases T $\beta$ RII levels, and stimulates collagen and CCN2 expression [27,57]. These data indicate that dermal fibroblasts in aged human skin retain their capacity to up-regulate the TGF- $\beta$  pathway and produce collagen. Thus, loss of structural integrity of the dermal ECM, with concomitant reduced attachment and actin cytoskeleton disassembly, may be drive the decline of collagen production by fibroblasts in aged human skin.

In summary, we report that disassembly of actin cytoskeleton leads to down-regulation of type I collagen via impairment of TGF- $\beta$ /Smad signaling. Actin cytoskeleton disassembly up-regulates miR-21, which in turn impairs TGF- $\beta$  signaling via specific down-regulation of T $\beta$ RII. These findings provide mechanistic insight regarding reduced expression of T $\beta$ RII and type I collagen, which are observed in aged human skin (Figure 5g).

#### **Author contribution**

ZQ performed the experiments and analyzed the data; TQ and GJF designed the experiments and wrote the manuscript; GJF and JJV discussed the analyses, interpretation, and edited the manuscript.

#### **Acknowledgements**

We thank Suzan Rehbine for the procurement of tissue specimens and Diane Fiolek for graphics and administrative assistance. This work was supported by the National Institute of Health (AG19364 to GJ Fisher and T Quan).

#### **Disclosure**

The authors declare no competing interests that might be perceived to influence the results and discussion reported in this paper.

#### **References**

1. Andreotti L, Bussotti A, Cammelli D, Aiello E, Sampognaro S. Connective tissue in aging lung. *Gerontology*. 1983; 29: 377-87.

2. **Jacob MP.** Extracellular matrix remodeling and matrix metalloproteinases in the vascular wall during aging and in pathological conditions. *Biomed Pharmacother.* 2003; 57: 195-202.
3. **Uitto J.** Connective tissue biochemistry of the aging dermis. Age-related alterations in collagen and elastin. *Dermatol Clin.* 1986; 4: 433-46.
4. **Yaar M, Gilchrest BA.** Skin aging: postulated mechanisms and consequent changes in structure and function. *Clin Geriatr Med.* 2001; 17: 617-30, v.
5. **Quan T, Fisher GJ.** Role of Age-Associated Alterations of the Dermal Extracellular Matrix Microenvironment in Human Skin Aging: A Mini-Review. *Gerontology.* 2015; 61: 427-34.
6. **Fisher GJ, Varani J, Voorhees JJ.** Looking older: fibroblast collapse and therapeutic implications. *Arch Dermatol.* 2008; 144: 666-72.
7. **Naylor EC, Watson RE, Sherratt MJ.** Molecular aspects of skin ageing. *Maturitas.* 2011; 69: 249-56.
8. **Smith JG, Jr., Davidson EA, Sams WM, Jr., Clark RD.** Alterations in human dermal connective tissue with age and chronic sun damage. *J Invest Dermatol.* 1962; 39: 347-50.
9. **Quan T, Shao Y, He T, Voorhees JJ, Fisher GJ.** Reduced expression of connective tissue growth factor (CTGF/CCN2) mediates collagen loss in chronologically aged human skin. *J Invest Dermatol.* 2010; 130: 415-24.
10. **Ashcroft GS, Horan MA, Ferguson MW.** The effects of ageing on cutaneous wound healing in mammals. *J Anat.* 1995; 187 ( Pt 1): 1-26.
11. **Gilchrest BA, Stoff JS, Soter NA.** Chronologic aging alters the response to ultraviolet-induced inflammation in human skin. *J Invest Dermatol.* 1982; 79: 11-5.
12. **Eaglstain WH.** Wound healing and aging. *Clin Geriatr Med.* 1989; 5: 183-8.
13. **Thomas DR.** Age-related changes in wound healing. *Drugs Aging.* 2001; 18: 607-20.
14. **Ashcroft GS, Mills SJ, Ashworth JJ.** Ageing and wound healing. *Biogerontology.* 2002; 3: 337-45.
15. **Rogers HW, Weinstock MA, Feldman SR, Coldiron BM.** Incidence Estimate of Nonmelanoma Skin Cancer (Keratinocyte Carcinomas) in the US Population, 2012. *JAMA Dermatol.* 2015; 151: 1081-6.
16. **Pickup MW, Mouw JK, Weaver VM.** The extracellular matrix modulates the hallmarks of cancer. *EMBO Rep.* 2014; 15: 1243-53.
17. **Fisher GJ, Quan T, Purohit T, Shao Y, Cho MK, He T, Varani J, Kang S, Voorhees JJ.** Collagen fragmentation promotes oxidative stress and elevates matrix metalloproteinase-1 in fibroblasts in aged human skin. *Am J Pathol.* 2009; 174: 101-14.
18. **Varani J, Schuger L, Dame MK, Leonard C, Fligel SE, Kang S, Fisher GJ, Voorhees JJ.** Reduced fibroblast interaction with intact collagen as a mechanism for depressed collagen synthesis in photodamaged skin. *J Invest Dermatol.* 2004; 122: 1471-9.
19. **Quan T, Little E, Quan H, Qin Z, Voorhees JJ, Fisher GJ.** Elevated matrix metalloproteinases and collagen fragmentation in photodamaged human skin: impact of altered extracellular matrix microenvironment on dermal fibroblast function. *J Invest Dermatol.* 2013; 133: 1362-6.

20. **Qin Z, Voorhees JJ, Fisher GJ, Quan T.** Age-associated reduction of cellular spreading/mechanical force up-regulates matrix metalloproteinase-1 expression and collagen fibril fragmentation via c-Jun/AP-1 in human dermal fibroblasts. *Aging Cell.* 2014; 13: 1028-37.
21. **Alenghat FJ, Nauli SM, Kolb R, Zhou J, Ingber DE.** Global cytoskeletal control of mechanotransduction in kidney epithelial cells. *Exp Cell Res.* 2004; 301: 23-30.
22. **Ingber DE.** Cellular mechanotransduction: putting all the pieces together again. *FASEB J.* 2006; 20: 811-27.
23. **Silver FH, Siperko LM, Seehra GP.** Mechanobiology of force transduction in dermal tissue. *Skin Res Technol.* 2003; 9: 3-23.
24. **Hynes RO.** The extracellular matrix: not just pretty fibrils. *Science.* 2009; 326: 1216-9.
25. **Geiger B, Spatz JP, Bershadsky AD.** Environmental sensing through focal adhesions. *Nat Rev Mol Cell Biol.* 2009; 10: 21-33.
26. **Fisher GJ, Shao Y, He T, Qin Z, Perry D, Voorhees JJ, Quan T.** Reduction of fibroblast size/mechanical force down-regulates TGF-beta type II receptor: implications for human skin aging. *Aging Cell.* 2016; 15: 67-76.
27. **Quan T, Wang F, Shao Y, Rittie L, Xia W, Orringer JS, Voorhees JJ, Fisher GJ.** Enhancing structural support of the dermal microenvironment activates fibroblasts, endothelial cells, and keratinocytes in aged human skin in vivo. *J Invest Dermatol.* 2013; 133: 658-67.
28. **Olson EN, Nordheim A.** Linking actin dynamics and gene transcription to drive cellular motile functions. *Nat Rev Mol Cell Biol.* 2010; 11: 353-65.
29. **Butcher DT, Alliston T, Weaver VM.** A tense situation: forcing tumour progression. *Nat Rev Cancer.* 2009; 9: 108-22.
30. **Mammoto T, Mammoto A, Ingber DE.** Mechanobiology and developmental control. *Annu Rev Cell Dev Biol.* 2013; 29: 27-61.
31. **Verrecchia F, Mauviel A.** Transforming growth factor-beta signaling through the Smad pathway: role in extracellular matrix gene expression and regulation. *J Invest Dermatol.* 2002; 118: 211-5.
32. **Quan T, He T, Shao Y, Lin L, Kang S, Voorhees JJ, Fisher GJ.** Elevated cysteine-rich 61 mediates aberrant collagen homeostasis in chronologically aged and photoaged human skin. *Am J Pathol.* 2006; 169: 482-90.
33. **Coue M, Brenner SL, Spector I, Korn ED.** Inhibition of actin polymerization by latrunculin A. *FEBS Lett.* 1987; 213: 316-8.
34. **Yarmola EG, Somasundaram T, Boring TA, Spector I, Bubb MR.** Actin-latrunculin A structure and function. Differential modulation of actin-binding protein function by latrunculin A. *J Biol Chem.* 2000; 275: 28120-7.
35. **Quan T, He T, Voorhees JJ, Fisher GJ.** Ultraviolet irradiation blocks cellular responses to transforming growth factor-beta by down-regulating its type-II receptor and inducing Smad7. *J Biol Chem.* 2001; 276: 26349-56.

36. **He T, Quan T, Shao Y, Voorhees JJ, Fisher GJ.** Oxidative exposure impairs TGF-beta pathway via reduction of type II receptor and SMAD3 in human skin fibroblasts. *Age (Dordr)*. 2014; 36: 9623.
37. **Gieni RS, Hendzel MJ.** Mechanotransduction from the ECM to the genome: are the pieces now in place? *J Cell Biochem*. 2008; 104: 1964-87.
38. **Dupont S, Morsut L, Aragona M, Enzo E, Giulitti S, Cordenonsi M, Zanconato F, Le Digabel J, Forcato M, Bicciato S, Elvassore N, Piccolo S.** Role of YAP/TAZ in mechanotransduction. *Nature*. 2011; 474: 179-83.
39. **Cai S, Liu X, Glasser A, Volberg T, Filla M, Geiger B, Polansky JR, Kaufman PL.** Effect of latrunculin-A on morphology and actin-associated adhesions of cultured human trabecular meshwork cells. *Mol Vis*. 2000; 6: 132-43.
40. **Giancotti FG, Ruoslahti E.** Integrin signaling. *Science*. 1999; 285: 1028-32.
41. **Miranti CK, Brugge JS.** Sensing the environment: a historical perspective on integrin signal transduction. *Nat Cell Biol*. 2002; 4: E83-90.
42. **Mazia D, Schatten G, Sale W.** Adhesion of cells to surfaces coated with polylysine. Applications to electron microscopy. *J Cell Biol*. 1975; 66: 198-200.
43. **Yu Y, Kanwar SS, Patel BB, Oh PS, Nautiyal J, Sarkar FH, Majumdar AP.** MicroRNA-21 induces stemness by downregulating transforming growth factor beta receptor 2 (TGFbetaR2) in colon cancer cells. *Carcinogenesis*. 2012; 33: 68-76.
44. **Kim YJ, Hwang SJ, Bae YC, Jung JS.** MiR-21 regulates adipogenic differentiation through the modulation of TGF-beta signaling in mesenchymal stem cells derived from human adipose tissue. *Stem Cells*. 2009; 27: 3093-102.
45. **Varani J, Dame MK, Rittie L, Fligel SE, Kang S, Fisher GJ, Voorhees JJ.** Decreased collagen production in chronologically aged skin: roles of age-dependent alteration in fibroblast function and defective mechanical stimulation. *Am J Pathol*. 2006; 168: 1861-8.
46. **Pohlers D, Brenmoehl J, Loffler I, Muller CK, Leipner C, Schultze-Mosgau S, Stallmach A, Kinne RW, Wolf G.** TGF-beta and fibrosis in different organs - molecular pathway imprints. *Biochim Biophys Acta*. 2009; 1792: 746-56.
47. **Varga J.** Scleroderma and Smads: dysfunctional Smad family dynamics culminating in fibrosis. *Arthritis Rheum*. 2002; 46: 1703-13.
48. **Boyd FT, Massague J.** Transforming growth factor-beta inhibition of epithelial cell proliferation linked to the expression of a 53-kDa membrane receptor. *J Biol Chem*. 1989; 264: 2272-8.
49. **Roberts A, Sporn M.** Peptide growth factors and their receptors. In: Sporn M, Roberts AB, editors. *Handbook of Experimental Pharmacology*. New York: Springer-Verlag New York Inc, 1990. p. 419-72.
50. **Cheifetz S, Massague J.** Transforming growth factor-beta (TGF-beta) receptor proteoglycan. Cell surface expression and ligand binding in the absence of glycosaminoglycan chains. *J Biol Chem*. 1989; 264: 12025-8.

51. **Qian SW, Burmester JK, Tsang ML, Weatherbee JA, Hinck AP, Ohlsen DJ, Sporn MB, Roberts AB.** Binding affinity of transforming growth factor-beta for its type II receptor is determined by the C-terminal region of the molecule. *J Biol Chem.* 1996; 271: 30656-62.
52. **Quan T, He T, Kang S, Voorhees JJ, Fisher GJ.** Solar ultraviolet irradiation reduces collagen in photoaged human skin by blocking transforming growth factor-beta type II receptor/Smad signaling. *Am J Pathol.* 2004; 165: 741-51.
53. **Gaspar P, Tapon N.** Sensing the local environment: actin architecture and Hippo signalling. *Curr Opin Cell Biol.* 2014; 31: 74-83.
54. **Fujita S, Ito T, Mizutani T, Minoguchi S, Yamamichi N, Sakurai K, Iba H.** miR-21 Gene expression triggered by AP-1 is sustained through a double-negative feedback mechanism. *J Mol Biol.* 2008; 378: 492-504.
55. **Lo YY, Wong JM, Cruz TF.** Reactive oxygen species mediate cytokine activation of c-Jun NH2-terminal kinases. *J Biol Chem.* 1996; 271: 15703-7.
56. **Quan C, Cho MK, Perry D, Quan T.** Age-associated reduction of cell spreading induces mitochondrial DNA common deletion by oxidative stress in human skin dermal fibroblasts: implication for human skin connective tissue aging. *J Biomed Sci.* 2015; 22: 62.
57. **Wang F, Garza LA, Kang S, Varani J, Orringer JS, Fisher GJ, Voorhees JJ.** In vivo stimulation of de novo collagen production caused by cross-linked hyaluronic acid dermal filler injections in photodamaged human skin. *Arch Dermatol.* 2007; 143: 155-63.

## Figure Legend

**Figure 1. Actin cytoskeleton disassembly down-regulates TGF- $\beta$  type II receptor.** Dermal fibroblasts were treated with Lat-A (30 nM) or DMSO (CTRL) for 24 hours. **(a)** Dermal fibroblasts were stained with phalloidin and imaged by fluorescence microscopy. Red fluorescence delineates cell cytoplasm; blue fluorescence delineates nuclei. The relative cell surface areas were quantified by ImageJ software. Arrow heads indicate stretched actin fibers. Mean  $\pm$  SEM, N =6, \*p<0.05 vs CTRL. Scale bars = 100  $\mu$ m. **(b)** mRNA levels of TGF- $\beta$  pathway components were quantified by real-time RT-PCR and normalized to the housekeeping gene 36B4. Mean  $\pm$  SEM, N=3, \*p<0.05 vs CTRL. **(c)** T $\beta$ RI and T $\beta$ RII protein levels were determined by Western blot and normalized to  $\beta$ -actin (loading control). Band intensities were quantified by MolecularImager. Inset shows representative Western blot. Mean  $\pm$  SEM, N=3, \*p<0.05 vs CTRL.



**Figure 2. Actin cytoskeleton disassembly down-regulates TGF- $\beta$ /Smad signaling and TGF- $\beta$  regulated type I procollagen and CCN2 expression.** Dermal fibroblasts were treated with Lat-A (30 nM) or DMSO (control) for 24 hours. **(a)** Smad2/Smad3 phosphorylation. Cells were treated with TGF- $\beta$ 1 (5ng/ml) for one hour. N=3, \*p<0.05 vs CTRL with TGF- $\beta$ 1. **(b)** Type I procollagen mRNA levels. Mean  $\pm$  SEM. N=3, \*p<0.05. **(c)** Type I procollagen protein levels. Mean  $\pm$  SEM, N=3, \*p<0.05. **(d)** CCN2 mRNA levels. Mean  $\pm$  SEM. N=3, \*p<0.05. **(e)** CCN2 protein levels. Mean  $\pm$  SEM, N=3, \*p<0.05. **(f)** Cells were cultured in type I collagen lattices, stained with phalloidin and imaged by fluorescence microscopy. Red fluorescence delineates cell cytoplasm; blue fluorescence delineates nuclei. Arrow heads indicate stretched actin fibers. Representative image of three independent experiments. Scale bar = 100  $\mu$ m. **(g)** Type I procollagen and CCN2 mRNA levels. Mean  $\pm$  SEM. N=3, \*p<0.05 vs CTRL. **(h)** Type I procollagen and CCN2 protein levels. Mean  $\pm$  SEM. N=3, \*p<0.05 vs CTRL. mRNA levels were quantified by real-time RT-PCR and normalized to the housekeeping gene 36B4. Protein levels were determined by Western blot analysis and normalized by  $\beta$ -actin (loading control). Band intensities were quantified by MolecularImager. Inset shows representative Western blot.

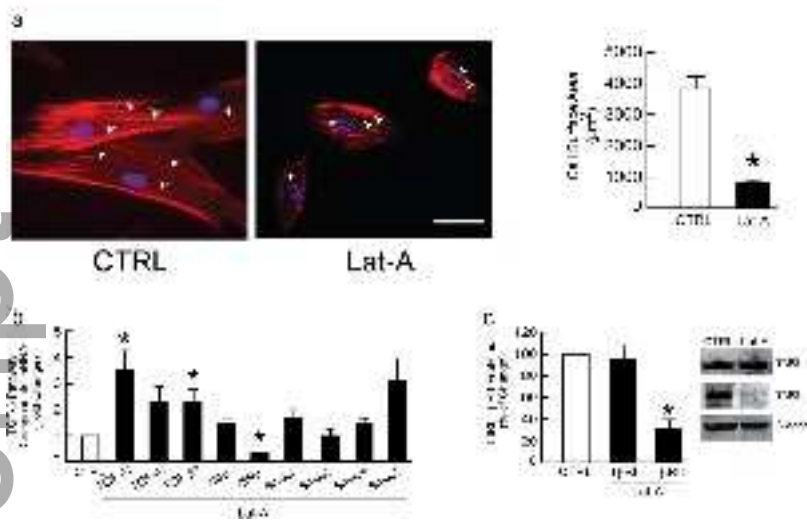
**Figure 3. Actin cytoskeleton assembly stimulates TGF- $\beta$  signaling and type I procollagen expression.** Dermal fibroblasts were treated with Lat-A (30 nM) or DMSO (control) for 24 hours. Lat-A-containing media was withdrawn 24 hours after its addition, followed by extensive washing with PBS and addition of fresh culture media. The cells were incubated for another 24 hours after removal of Lat-A **(a)** Cells were stained with phalloidin (red) to image the actin cytoskeleton and DAPI (blue) to image nuclei. The relative cell surface areas were quantified by ImageJ software. Arrow heads indicate stretched actin fibers. Mean  $\pm$  SEM, N =6, \*p<0.05. Scale bar = 100  $\mu$ m. **(b)** T $\beta$ RII protein levels. Mean  $\pm$  SEM, N =4, \*p<0.05. **(c)** Smad2/Smad3 phosphorylation. Cells were treated with TGF- $\beta$ 1 (5ng/ml) for one hour. **(d)** Type I procollagen (Col-1) and CCN2 protein levels. Mean  $\pm$  SEM, N =3, \*p<0.05 vs CTRL. Protein levels were determined by Western blot analysis and normalized to  $\beta$ -actin (loading control). Band intensities were quantified by MolecularImager. Inset shows representative Western blot.

**Figure 4. Down-regulation of T $\beta$ RII mediates impaired TGF- $\beta$  signaling and type I procollagen production by actin cytoskeleton disassembly.** (a) Knockdown of T $\beta$ RII expression by T $\beta$ RII siRNA. Cells were transfected with control siRNA or T $\beta$ RII siRNA. Two days, cells were treated with vehicle or TGF- $\beta$ 1 (5ng/ml) for one hour. T $\beta$ RII and Smad3 phosphorylation (p-Smad3) was determined by Western blot. Protein levels were normalized to  $\beta$ -actin (loading control). Band intensities were quantified by MolecularImager. Inset shows representative Western blot. Mean  $\pm$  SEM, N =3, \*p<0.05 vs CTRL. (b) Dermal fibroblasts were treated with Lat-A (30 nM) or DMSO (control, CTRL) for 24 hours. Culture media were removed 24 hours later, followed by extensive washing with PBS and replacement with fresh media alone (Lat-A withdrawal) or containing Lat-A. Cells were transfected with control siRNA or T $\beta$ RII siRNA, as indicated. Twenty-four hours later, cells were treated with vehicle or TGF- $\beta$ 1 (5ng/ml) for one hour. Smad3 phosphorylation (p-Smad3) was determined by immunostaining (red). Nuclei were stained with DAPI (blue). Scale bars = 100  $\mu$ m. (c) Fibroblasts were transfected with T $\beta$ RII expression vector, and 48 hours later treated with Lat-A (30 nM) for 24 hours. Cells were stained for T $\beta$ RII (green) and type I procollagen (Col-1, red, top row), or CCN2 (red, lower row) by immunofluorescence. Nuclei were stained with DAPI (blue). Arrow heads indicate cells with reduced T $\beta$ RII. Of note, these cells also displayed reduced expression of Col-1 and CCN2. Scale bars = 100  $\mu$ m. (d) Cells were transfected with control vector or T $\beta$ RII expression vector for 48 hours, then treated with vehicle or Lat-A (30 nM) for 24 hours. The actin cytoskeleton was stained with phalloidin (red) and imaged by fluorescence microscopy. Nuclei were stained with DAPI. Arrow heads indicate stretched actin fibers. All images are representative of three independent experiments. Scale bars = 100  $\mu$ m.

**Figure 5. Actin cytoskeleton disassembly induces miR-21, which reduces T $\beta$ RII expression.** (a) miR-21 expression levels. Dermal fibroblasts were treated with Lat-A (30 nM) or DMSO (CTRL) for 24 hours. miR-21 levels were determined by real-time PCR and normalized to RNU6B, endogenous reference siRNA. Mean  $\pm$  SEM, N =3, \*p<0.05 vs CTRL. (b) T $\beta$ RII protein levels. Cells were transfected with control siRNA, miR-21 mimic, or miR-21 inhibitor for 48 hours. Protein levels were determined by capillary electrophoresis immunoassay. Mean  $\pm$  SEM, N =3, \*p<0.05 vs CTRL siRNA. (c) T $\beta$ RII protein levels. Cells were transfected with

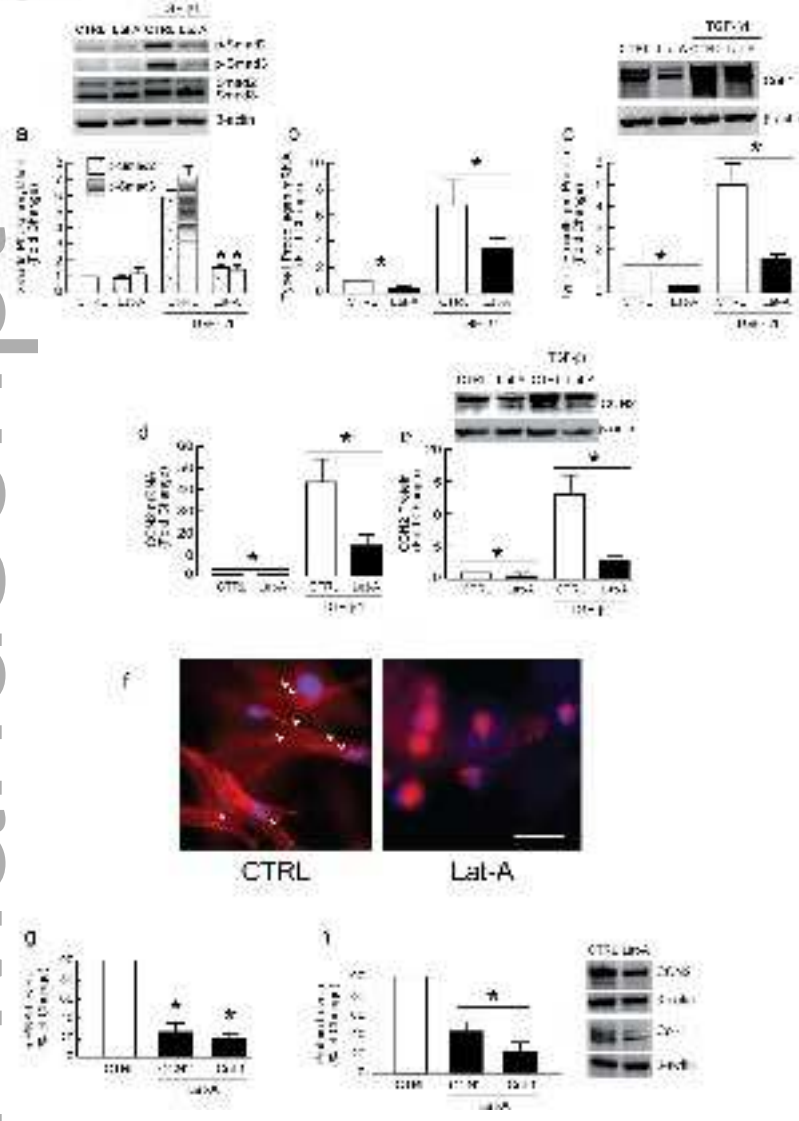
control siRNA or miR-21 inhibitor for 48 hours, then treated with Lat-A (30 nM) or DMSO (control) for 24 hours. Protein levels were determined by capillary electrophoresis immunoassay. Mean  $\pm$  SEM, N=3, \*p<0.05. **(d)** miR-21 mimic inhibits Smad3 phosphorylation. Cells were transfected with control siRNA or miR-21 mimic for two days. Cells were treated with vehicle or TGF- $\beta$ 1 (5ng/ml) for one hour. Smad3 phosphorylation was determined by capillary electrophoresis immunoassay. **(e)** miR-21 mimic inhibits Smad3 phosphorylation. Cells were transfected with control siRNA or miR-21 mimic for two days. Cells were treated with vehicle or TGF- $\beta$ 1 (5ng/ml) for one hour. Smad3 phosphorylation (p-Smad3) was determined by immunostaining (red). Nuclei were stained with DAPI (blue). Images are representative of three independent experiments. Scale bars = 25  $\mu$ m. **(f)** miR-21 mimic inhibits type I collagen and CCN2 expression. Cells were transfected with control siRNA or miR-21 mimic for two days. Type I procollagen and CCN2 protein levels were determined by Western blot and normalized to  $\beta$ -actin (loading control). Band intensities were quantified by MolecularImager. Inset shows representative Western blot. Mean  $\pm$  SEM, N =3, \*p<0.05 vs CTRL siRNA. Protein levels **(b-d)** were determined by capillary electrophoresis immunoassay and normalized to  $\beta$ -actin (loading control). Band intensities were quantified by Compass software. Inset shows representative digital images. **(g)** Diagram illustrating proposed mechanism of age-related skin thinning and fragility. Collagen fibril fragmentation, reduced fibroblast attachment, and actin cytoskeleton disassembly act in concert to up-regulate miR-21, which in turn impairs TGF- $\beta$  signaling via specific down-regulation of T $\beta$ RII. Impaired TGF- $\beta$  signaling reduces production of collagen and other ECM proteins, which eventuates in loss of dermal mass, giving rise to thin, fragile skin, a prominent feature of aged human skin.

Figure 1



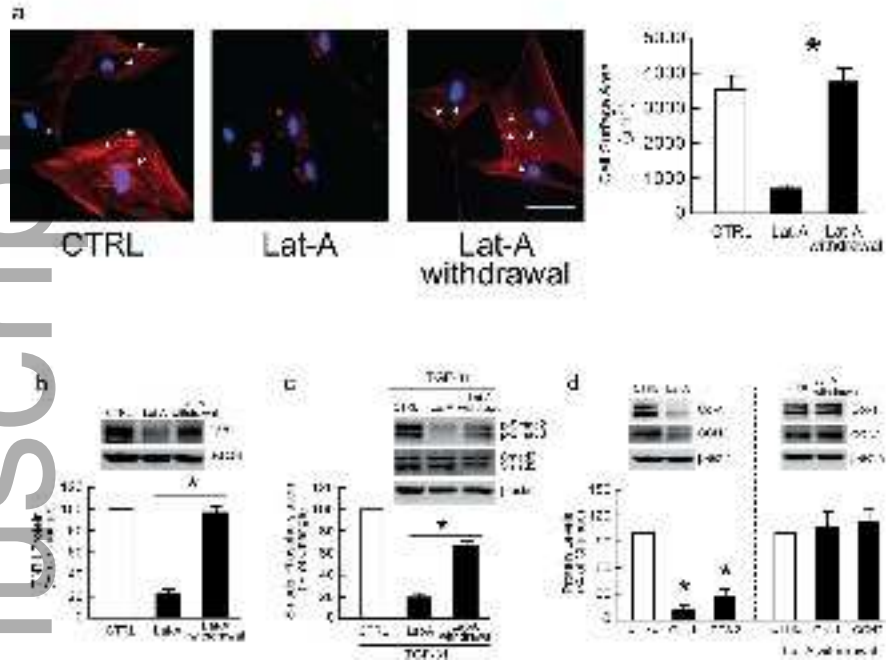
jcm1\_13685\_f1.tif

Figure 2



jcmm\_13685\_f2.tif

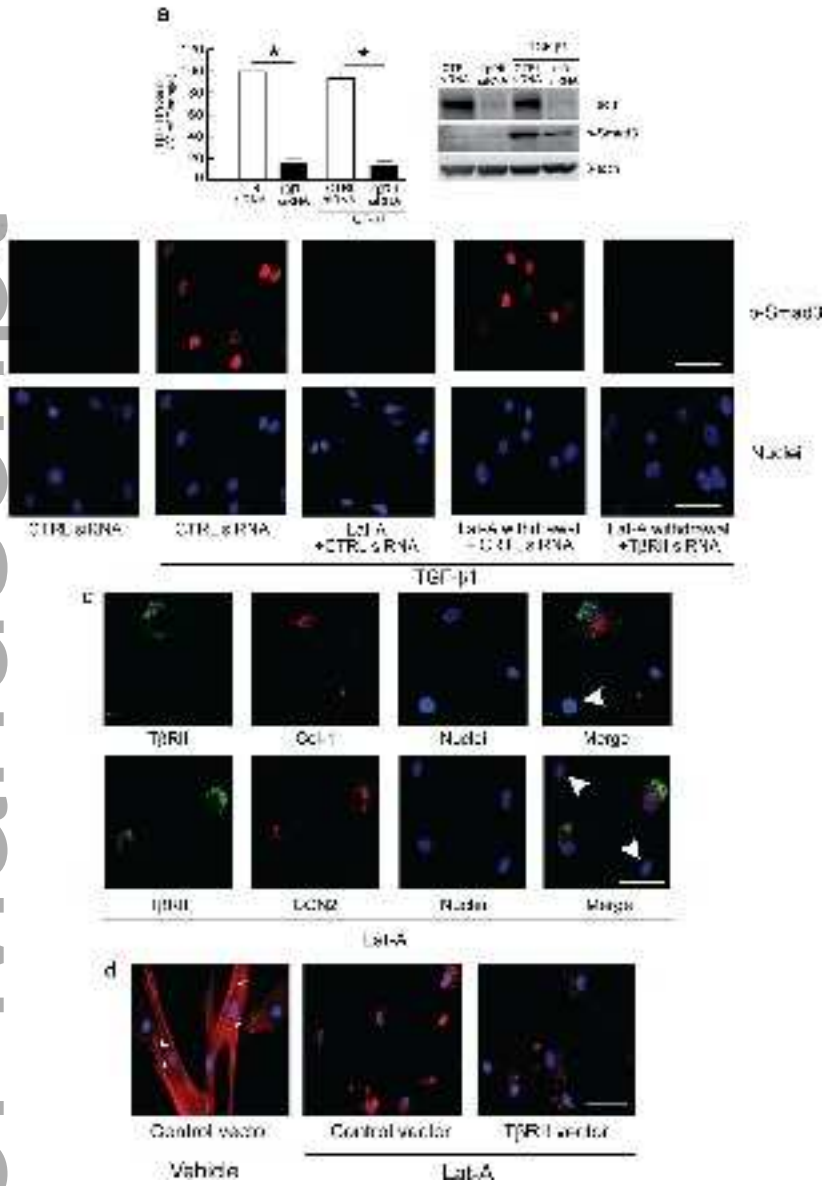
Figure 3



jcm\_13685\_f3.tif

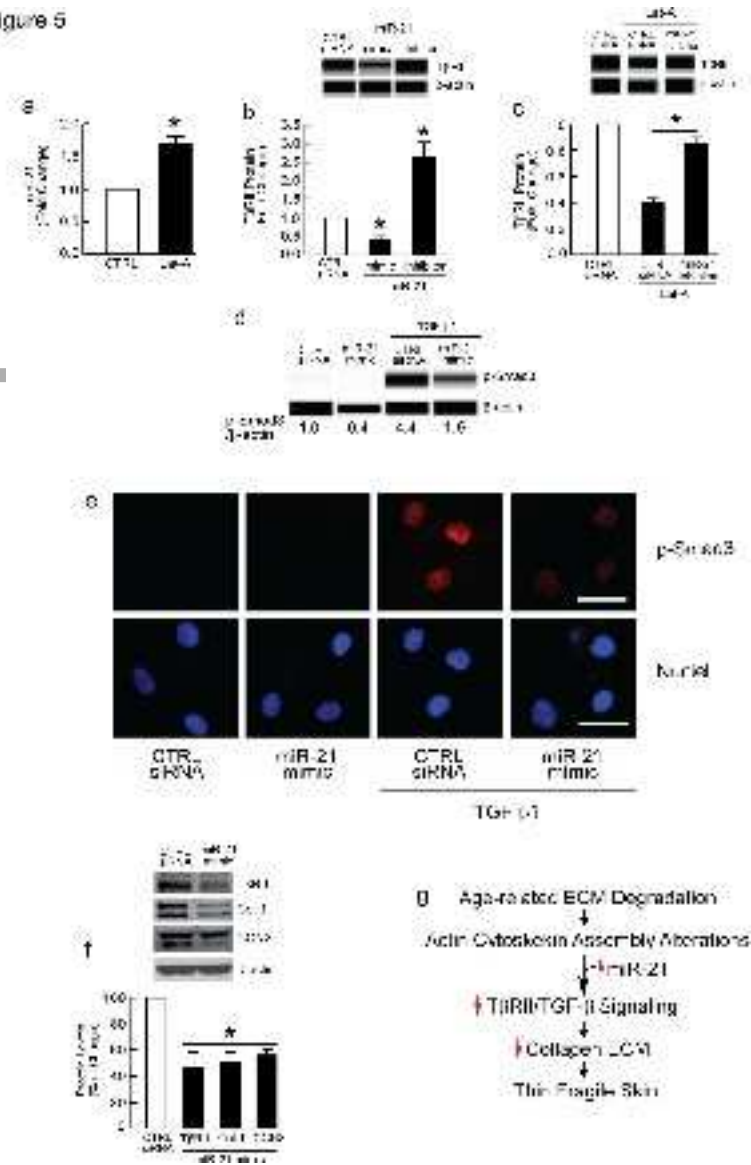
Figure 4

Author Manuscript



jcm\_13685\_f4.tif

Figure 5



jcm113685\_f5.tif